Arch. Mech., 46, 4, pp. 413–429, Warszawa 1994

Experimental and numerical investigations of thermal-mechanical behaviour of poly- and single-crystalline nickel-base superalloys

A. BERTRAM, J. OLSCHEWSKI and R. SIEVERT (BERLIN)

Dedicated to Professor Dr.-Ing. F. G. Kollmann on the occasion of his 60th birthday

THE LIFE-TIME assessment of structural components operating at high temperatures, such as e.g. gas turbines, requires an accurate prediction of the inelastic material response by appropriate constitutive models. The present paper shows some inelastic properties of particle hardened nickel-base superalloys, which are used as turbine blade materials, and their modelling by Chaboche's viscoplastic model and an anisotropic three-dimensional viscoelastic model. The simulation possibilities are demonstrated for non-isothermal uni- and multiaxial cyclic behaviour of an isotropic material and for creep behaviour of a cubic single crystal in comparison with the experimental findings.

1. Introduction

AN ADVANCED design methodology of gas turbines requires the use of materials with high-temperature capabilities and, in addition, a realistic assessment of stresses and strains in the highly stressed parts of the system. Among the most highly stressed components, turbine blades are submitted to high temperature and thermal stress cycles combined with centrifugal loads. To achieve maximum performance, the inelastic material behaviour must be taken into account. In general, materials used in high-temperature applications, as e.g. nickel-base superalloys, exhibit both short-term plastic deformation, long-term creep deformation, and the interaction between them. The material inelasticity and the normal service conditions containing multiaxial, cyclic and non-isothermal loading histories represent a challenge for the predictive capabilities of the constitutive models in question. For that purpose, unified constitutive models have been developed in the past.

In the first part of this paper, the viscoplastic CHABOCHE model [1] has been applied to predict the material response of the nickel-base superalloy IN738LC, a polycrystalline cast alloy used as blade material for stationary gas turbines. The prediction capabilities of the model will be demonstrated with respect to non-proportional and non-isothermal loadings.

The second part of this paper deals with the description of isothermal creep behaviour of the single-crystalline superalloy CMSX6. The use of single crystals as turbine blade materials has the advantage of a higher thermodynamic efficiency because of a higher gas entry-temperature and a better corrosion resistance compared with similar polycrystalline materials. They are used mainly in flight engines. The disadvantage, from the theoretical point of view, is the greater complexity of the material behaviour because of the anisotropy which has to be modelled. We will present a three-dimensional constitutive model based on the tensor function approach which exhibits the cubic symmetry of the material. Furthermore, we will demonstrate the model capabilities to describe the crystal orientation-dependent creep behaviour of the material.

Part A. Description of isotropic behaviour at high temperature

2. Constitutive model and isothermal loading

2.1. Viscoplastic theories

Modelling of the inelastic behaviour of nickel-base superalloys is a complex task. These materials show complicated deformation phenomena due to the various strengthening mechanisms caused by second phase particles which are not well understood at present. For example, a typical response of superalloys is the non-monotonous variation of the yield strength with temperature as reported by POPE and EZZ [2]. Regarding the alloy IN 738 LC, this particular behaviour is shown in Fig. 1a. A further complexity arises from the history-dependence of the material behaviour which is obviously influenced by creep-fatigue interaction processes. Strain-rate dependent materials exhibit the phenomenon that the relaxation response is different if the relaxation process starts under the same applied stress, but from different points of a hysteresis loop (see, e.g. ROBINSON [3]).

There is a vast literature on inelastic constitutive models capable for high temperature applications. In particular, the state variable viscoplastic or unified theories, using only one inelastic strain component, have proved their suitability. The description of creep-fatigue interaction is based on coupling of the inelastic strain with hardening variables changing during the inelastic process. A literature survey on viscoplastic models with a special emphasis on the hardening rules used has been given by KREMPL [4]. An overview on the predictive capabilities of further models used in engineering practice can be found in [5].

A widely accepted representative of the class of unified models is the viscoplastic CHABOCHE model [1] which has been selected for the present investigation. A comparison of models with different flow rules, as e.g. those of BODNER–PARTOM [6] and CHABOCHE [1], has demonstrated (see OLSCHEWSKI *et al.* [7]) that the prediction behaviour of both models is very similar if the model calibration procedure is performed very carefully. Differences occur only if the direction of the inelastic deformation is of importance, such as in relaxation processes under multiaxial loading, see the example plotted in Fig. 2. There is experimental evidence that the direction of inelastic strain-rate is not determined by the stress deviator alone.

2.2. Isothermal uni- and multiaxial loading

The Chaboche model valid at isothermal conditions is given in Table 1. The material parameters are constitutive functions of temperature. The values of these functions have been determined for several temperatures by using isothermal uniaxial tests only. For this purpose the material parameters are divided into groups with respect to different ranges of hardening behaviour (e.g. primary and cyclic hardening) and determined by a stepwise optimization procedure based on the Levenberg–Marquardt algorithm [8]. Only simple strain-controlled tensils and cyclic tests, as well as monotonous creep tests have been used. The result of this calibration procedure with respect to IN 738 LC is shown in Table 2.

Table 1. Evolution equations of Chaboche's model for isothermal processes.

Hooke's law

$$\mathbf{S} = \mathbf{C}(T)(\mathbf{E}_m - \mathbf{E}_i), \quad \mathbf{E}_m := \mathbf{E} - \mathbf{E}_{\text{th}}(T), \quad \mathbf{E}_{\text{th}} = \alpha(T)(T - T_0)\mathbf{1}. \tag{2.1}$$

Flow rule

$$\dot{\mathbf{E}}_i = \sqrt{\frac{3}{2}}\left\langle \frac{J_2(\mathbf{S}' - \mathbf{X}) - R_y}{K} \right\rangle^n \frac{\mathbf{S}' - \mathbf{X}}{\|\mathbf{S}' - \mathbf{X}\|}, \tag{2.2}$$

$$\langle y \rangle := \begin{cases} y, & \text{if } y > 0 \\ 0, & \text{if } y \leq 0, \end{cases} \qquad J_2(-) := \sqrt{\frac{3}{2}}\|(-)\|.$$

Hardening rules

isotropic

$$\dot{R}_y = b(R_{y\infty} - R_y)\dot{p}, \quad \dot{p} = \sqrt{\frac{2}{3}}\|\dot{\mathbf{E}}_i\|, \quad R_y(t = 0) = k, \tag{2.3}$$

kinematical

$$\dot{\mathbf{X}} = c\left(a\frac{\mathbf{S}' - \mathbf{X}}{J_2(\mathbf{S}' - \mathbf{X})} - \phi(p)\mathbf{X}\right)\dot{p} - d\left(\frac{J_2(\mathbf{X})}{a}\right)^r \frac{\mathbf{X}}{J_2(\mathbf{X})},$$

$$\phi(p) = \phi_\infty - (\phi_\infty - 1)e^{-\omega p}. \tag{2.4}$$

$\mathbf{E}$	total strain tensor at small deformations,
$\mathbf{E}_{th}, \mathbf{E}_m, \mathbf{E}_i$	thermal, mechanical and inelastic strain tensor,
$\mathbf{S}, \mathbf{S}'$	stress tensor and the deviator,
$\mathbf{C}$	elastic stiffness tensor of 4th order,
$\mathbf{X}$	internal stress tensor of induced anisotropy,
$\|\ \|$	Euclidean norm,
R_y	isotropic internal stress,
p	accumulated inelastic strain.

Table 2. Material parameters of Chaboche's model for IN 738 LC.

IN 738 LC	RT	450° C	600° C	750° C	850° C	950° C
E [MPa]	197 570.	188 550.	166 230.	152 450.	149 650.	139 370.
ϑ	0.33	0.33	0.33	0.33	0.33	0.33
K	111.	39.	84.	1166.	1150.	790.
n	8.6	10.	10.	5.9	7.7	6.8
k [MPa]	580.	460.	543.	330.	153.	79.
$R_{y\infty}$ [MPa]	439.	349.	554.	237.	0.	0.
b	17.	17.	13.	16.	317.	439.
a [MPa]	277.	234.	210.	319.	311.	188.
c	862.	1207.	724.	499.	201.	267.
ϕ_∞	0.47	0.36	0.46	0.73	1.	1.
ω	18.3	40.6	34.7	12.	(0.)	–
d [MPa/s]	0.	0.	$3.5 \cdot 10^{-3}$	$3.5 \cdot 10^{-3}$	$2.3 \cdot 10^{-2}$	$9 \cdot 10^{-2}$
r	–	(4.)	4.2	1.3	4.8	4.4

The material constants represent the typical temperature-dependence of the yield strength $R_{p0.2}$, Fig. 1a. At 750° C, IN 738 LC exhibits no strict monotonous strain-rate dependence as it is the case at 850° C and 950° C. At temperatures less than 600° C we have a quasi-strain-rate insensitivity. Therefore, relaxation tests instead of creep tests have been used in the calibration process at lower temperatures to check the remaining strain-rate dependence.

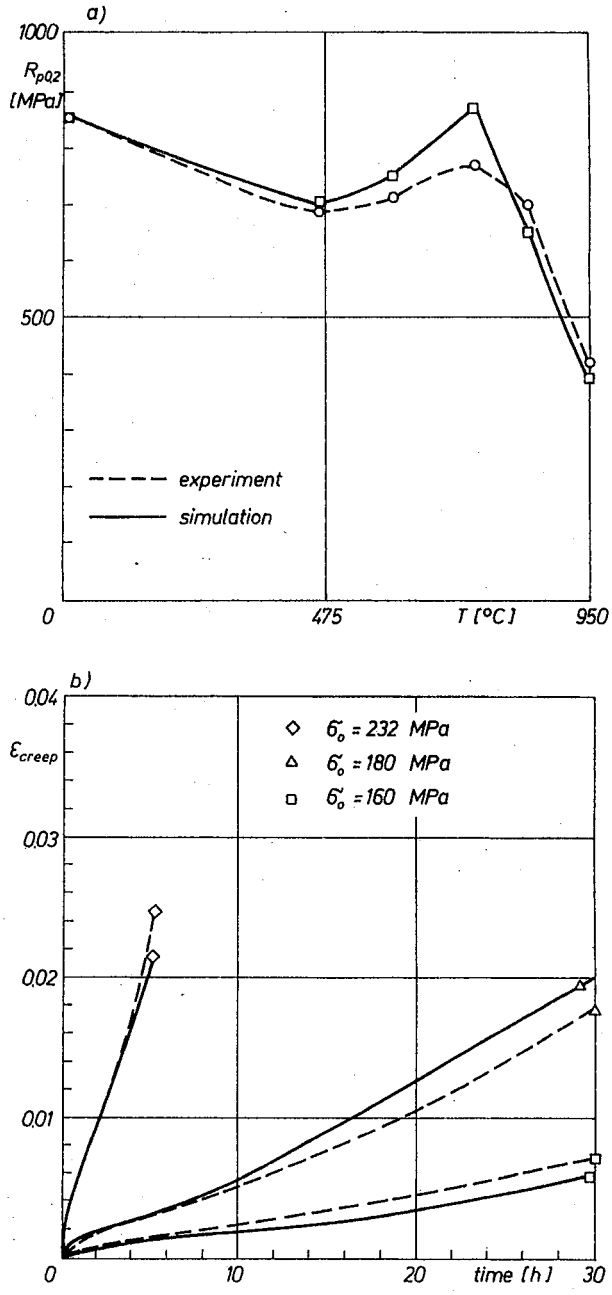

FIG. 1. Modelling of uniaxial behaviour: Temperature variation of the yield strength at $\dot{\varepsilon} = 10^{-3}$ s a), creep behaviour at 950° C b).

Fig. 1b shows primary and secondary creep behaviour at 950° C. An increasing creep-rate at constant load is connected with a decreasing flow resistance. The varying creep-rate, as indicated in Fig. 1b, is predicted by the model on the basis of a competition between

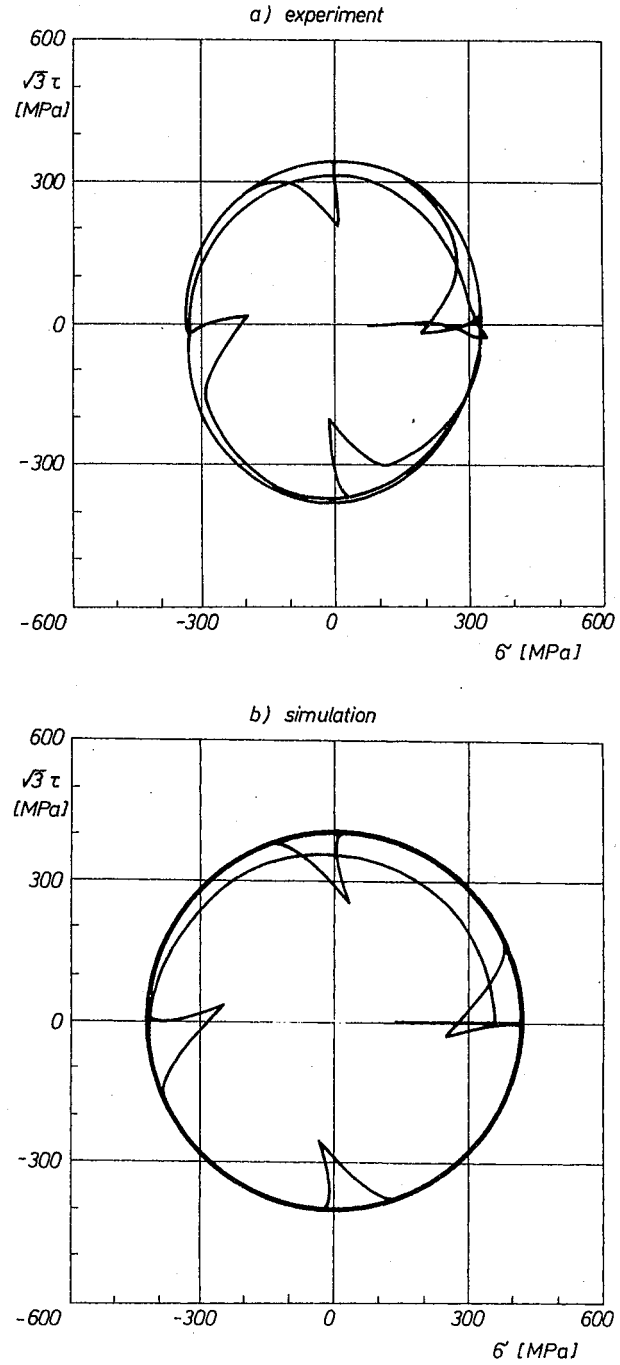

FIG. 2. Cyclic axial-torsional loading: Material response a) to a 90° out-of-phase straining with hold times at stress extrema (950° C, $\varepsilon_{eq} = 0.006$, $\dot{\varepsilon}_{eq} = 10^{-3}$ /s, $t_H = 120$ s) and its simulation b).

kinematical hardening and an isotropic softening which both converge to a certain limit but with different rates.

The behaviour of IN 738 LC under uniaxial cyclic loading at 850° C and 950° C is characterized by a stress saturation level which is reached after a few cycles, i.e. the material shows only a slight cyclic hardening. This observation leads to the values of the material parameters ϕ_∞ and ω of Table 2.

Figure 2 points out the multiaxial cyclic hardening behaviour at 950° C under a sinusoidal axial-torsional loading path where the axial and shear strain are controlled in 90° C — out-of-phase. This results in a circular strain path in the $\varepsilon - \gamma/\sqrt{3}$ plane. Hold times of strain were imposed at the peak stresses (ZIEBS *et al.* [9]). The material response in a saturated cycle, Fig. 2a, is simulated Chaboche's model which is calibrated to uniaxial behaviour only, Fig. 2b. As it is indicated in Fig. 2b, IN 738 LC exhibits no additional hardening under non-proportional cyclic loading either, at 950° C as well as at other temperatures. The same observation has been made for the isotropic particle hardened superalloy B1900+Hf (CHAN *et al.* [10]).

3. Non-isothermal loading

3.1. Model formulation

For isothermal loading, the rate equation of isotropic hardening, Eq. $(2.3)_1$, can be integrated to

$$R_y = \widehat{R}_y(p,T) := R_{y\infty}(T) - (R_{y\infty}(T) - k(T))e^{-b(T)p}. \tag{3.1}$$

As a generalization, this *finite state function* can be considered to be valid also in non-isothermal processes (BENALLAL and BEN CHEIKH [11], BHATTACHAR and STOUFFER [12]). Equivalent to Eq. (3.1) is the following incremental evolution equation:

$$\begin{aligned} \dot{R}_y &= \frac{\partial \widehat{R}_y}{\partial p}\dot{p} + \frac{\partial \widehat{R}_y}{\partial T}\dot{T}, \qquad R_y(t=0) = k(T_0), \\ &= b(R_{y\infty} - R_y)\dot{p} + \frac{\partial \widehat{R}_y}{\partial T}\dot{T}. \end{aligned} \tag{3.2}$$

Obviously, the finite state function, Eq. (3.1), corresponds to a *temperature-rate term* in the rate equation (MORENO and JORDAN [13]).

Equation (3.2) contains two limiting cases: At the beginning of the process, $p = 0$, R_y is equal to the initial internal stress, $R_y = k$, and the $\dot{T}$ — term reads (cf. SLAVIK and SEHITOGLU [14]):

$$\dot{R}_y = b(R_{y\infty} - R_y)\dot{p} + \frac{dk}{dT}\dot{T}. \tag{3.3}$$

In a saturated state, $p \to \infty$, the isotropic hardening variable $R := R_y - k$ has the evolution equation

$$\dot{R} = b(h - R)\dot{p} + \frac{dh}{dT}\dot{T}, \qquad h(T) := R_{y\infty}(T) - k(T). \tag{3.4}$$

This form has been enlarged to consider additional hardening under non-proportional multiaxial loading (BENALLAL and BEN CHEIKH [15], MCDOWELL [16]). But the cycling hardening behaviour of high-temperature alloys with relatively high volume fraction of so-called γ'-particles ($> 40\%$, IN 738 LC, B1900+Hf) under in-phase and out-of-phase loading is essentially the same.

In general, one has to take into account static recovery in the evolution equation for isotropic hardening (CHABOCHE [17]). Such a static recovery term could be added to the rate equation (3.2). Static recovery of the internal back-stress, last term of Eq. $(2.4)_1$, has been considered to be able to simulate the creep behaviour of Fig. 1b, for example. Static recovery of the isotropic internal stress (elastic region) which is present especially at the beginning of the process, can be important for the description of the material behaviour at very low strain-rates ($\dot{\varepsilon} < 10^{-7}$/s; cf. KREMPL [18]).

Calculations with a temperature-rate term in the kinematical hardening rule have not given any improvement of the simulation quality (cf. [19]). Therefore, only a $\dot{T}$-term in the isotropic hardening rule, Eq. (3.2), will be considered in the following section. The temperature functions of the material parameters are approximated by linear interpolation of the values obtained at certain temperatures, Table 2.

3.2. Non-isothermal uni- and multiaxial cyclic loading

Turbine blades are subjected to thermal-mechanical fatigue loading. Therefore it is necessary that the constitutive models should be able to predict non-isothermal stress-strain

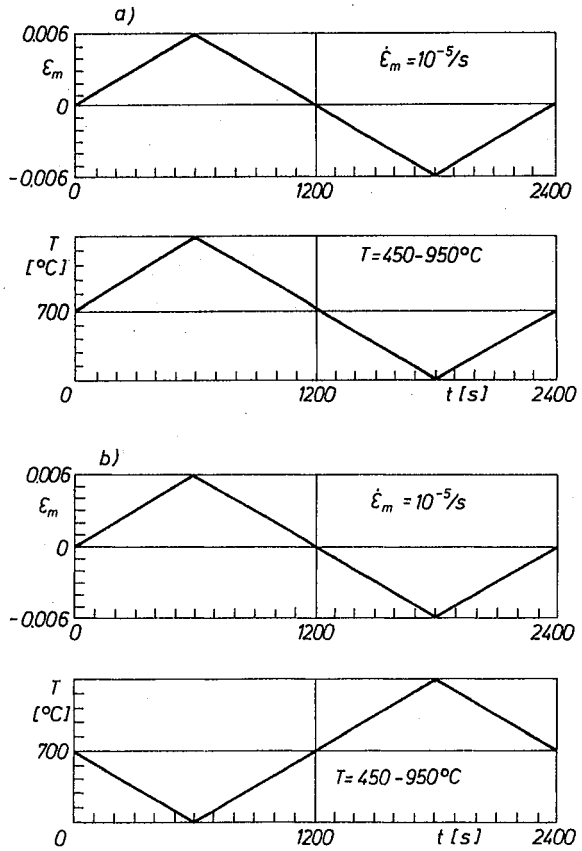

FIG. 3. Non-isothermal uniaxial cyclic loading: loading histories; in-phase a), out-of-phase b).

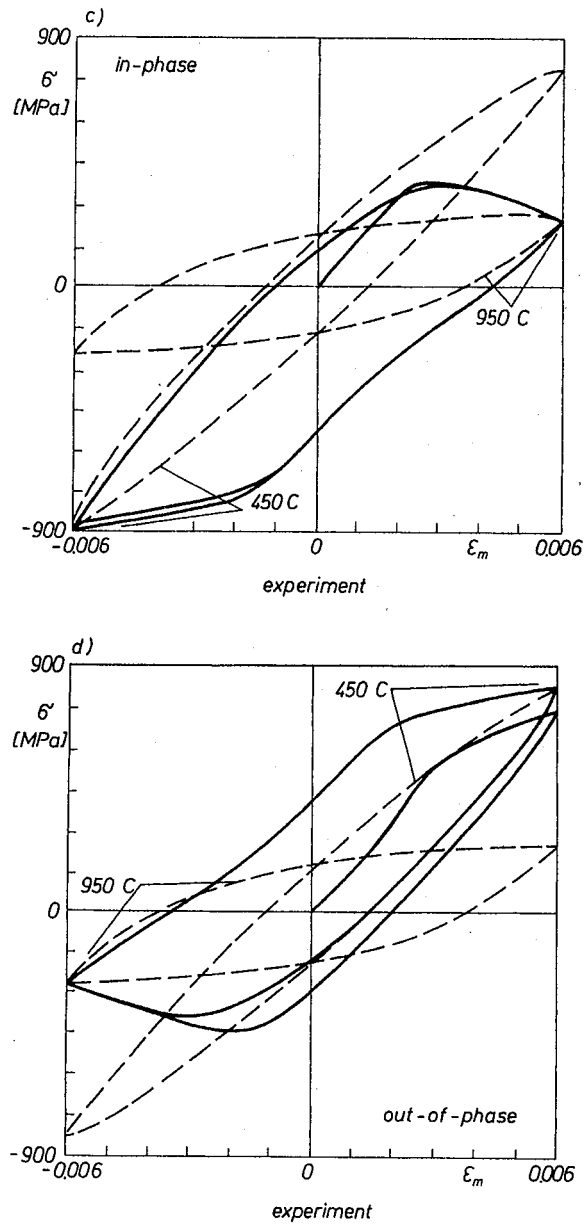

FIG. 3. Non-isothermal uniaxial cyclic loading: material response (c, d) $\dot{T} = 0.417°$ C/s; solid lines represent non-isothermal and dashed lines — the isothermal behaviour.

behaviour of the material. Especially in cooled turbine blades, where strong temperature gradients are present, thermal stresses are an important load. Relevant to the stress is the mechanical part of strain. Hence, in the experiments the mechanical strain is controlled simultaneously with temperature. In the testing machine, the total strain is applied in

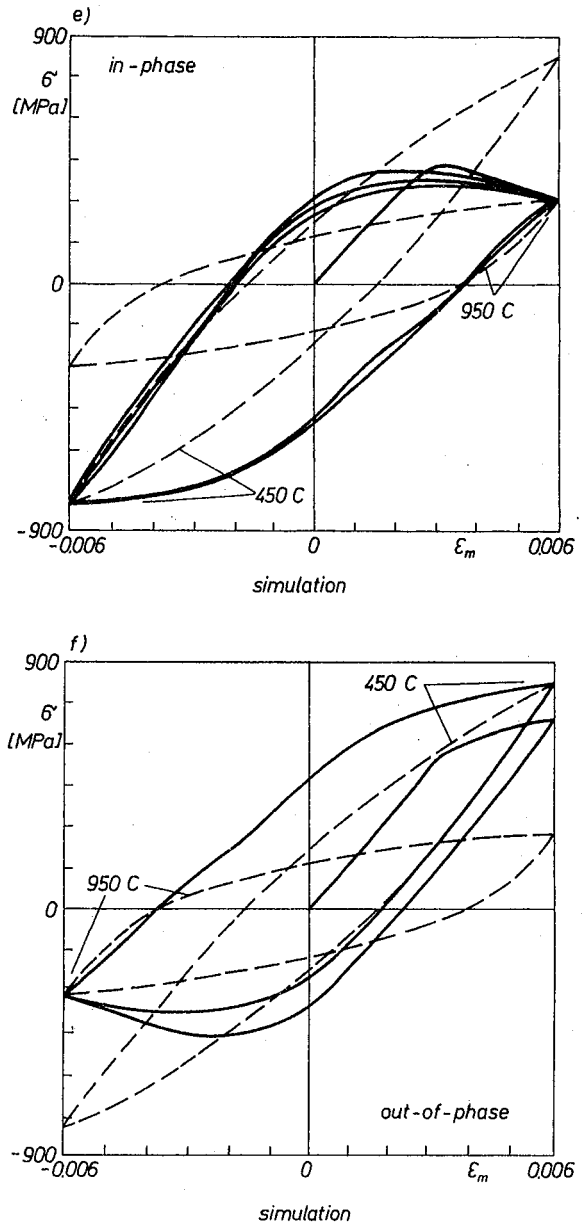

FIG. 3. Non-isothermal uniaxial cyclic loading: simulation (e, f) $\dot{T} = 0.417°$ C/s; solid lines represent non-isothermal and dashed lines — the isothermal behaviour.

such a way that the mechanical strain follows a given course in time, e.g. in-phase with temperature, Fig. 3a. At out-of-phase straining, Fig. 3b, the total strain does not have to be so large for compression and tension because of thermal expansion and shrinking, respectively.

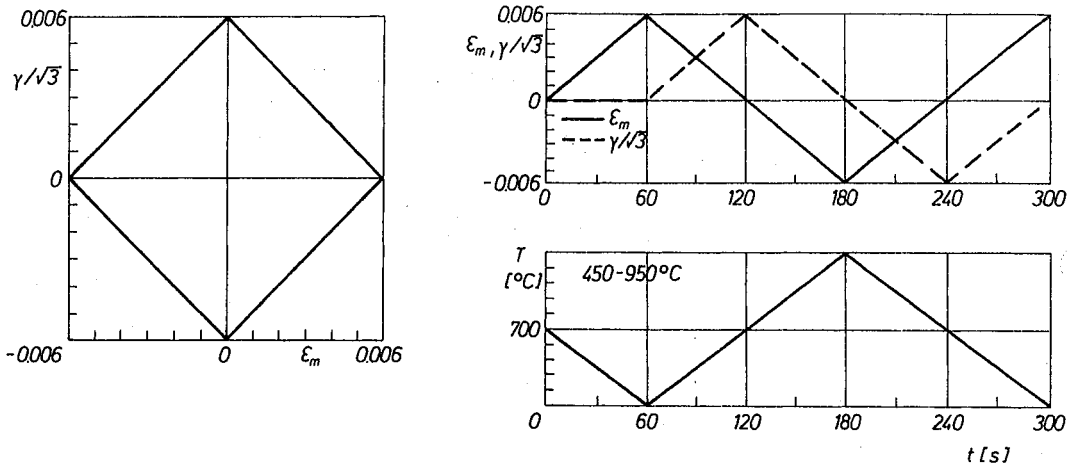

a)

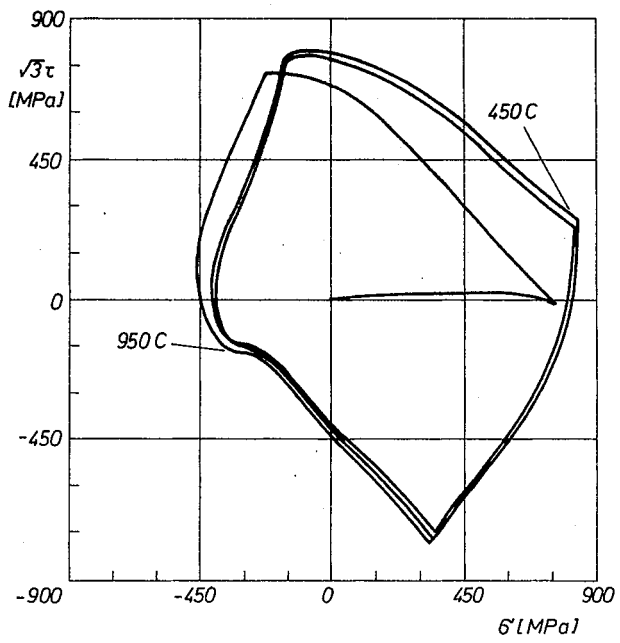

b) experiment

[Fig. 4.]

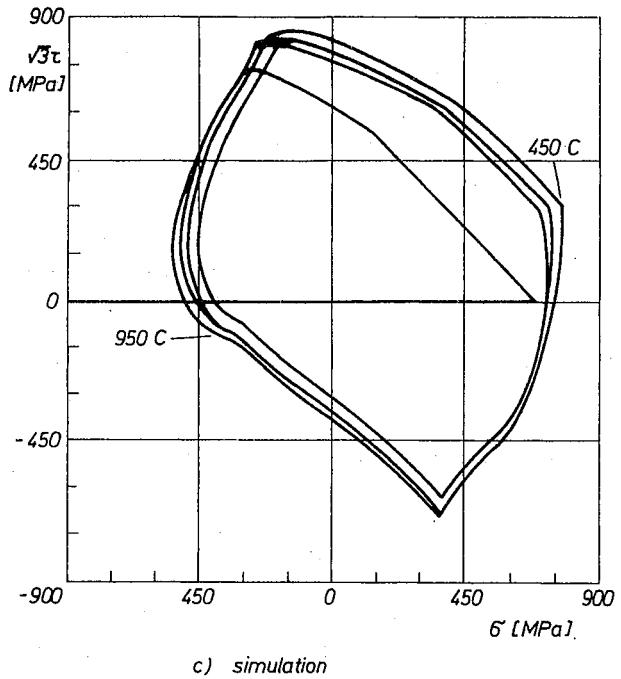

c) simulation

FIG. 4. Non-isothermal axial-torsional cyclic loading: Loading history a) $\dot{T} = 4.17°$ C/s, material response b) and simulation c).

The material response measured in these uniaxial tests is shown in Figs. 3c,d. The full lines correspond to the non-isothermal cyclic loading in the temperature interval between 450 and 950° C. The dashed lines represent the material behaviour under isothermal cyclic straining at the maximum and minimum temperature of the non-isothermal cycle, respectively. The resulting stress levels at the strain amplitudes in both non-isothermal loadings are of the same order as those of the associated isothermal loadings. This leads to asymmetric hysteresis loops under non-isothermal conditions.

Predictions based on Chaboche's model with an additional temperature-rate term in the isotropic hardening rule, as already discussed in Sect. 3.1, Eq. (3.2), reproduce these phenomena, Figs. 3e,f. The material constants, see Table 2, are determined exclusively by isothermal uniaxial tests. Neglecting the temperature-rate term which characterizes hardening or softening induced by temperature changes, the prediction would not meet the isothermal stress amplitudes, especially at the low temperature amplitude, [19]. With the introduced temperature-rate term or, equivalently, with the finite state function, Eq. (3.1), the model reaches instantaneously the yield strength R_y corresponding to the actual temperature.

A more complex stress state results under non-isothermal multiaxial loading. An example is shown in Fig. 4. The thermal-mechanical loading history is plotted in Fig. 4a. The axial strain/shear strain path is of diamond shape. The temperature is applied under 180° out-of-phase with respect to the axial strain. Figure 4b shows the material response to the non-isothermal axial-torsional cyclic loading. The simulation of the material behaviour is given in Fig. 4c. The model prediction shows all the characteristic features of

the material response as there are the curvature of the stress-path which is due to the varying hardening and stress extrema which do not correspond to the strain extrema.

From the rheological point of view Chaboche's viscoplastic theory is a Bingham-type model (LEMAITRE and CHABOCHE [20]). At high temperature viscous effects (relaxation and creep) are more important. Therefore, anisotropic creep will be described by a Burgers-type model in the second part of this paper.

Part B. Description of cubic anisotropic behaviour at high temperature

4. Creep modelling

4.1. Constitutive theories for single crystals

For single crystals the situation is quite different from that for polycrystalline materials, as the creep behaviour depends highly on the orientation of the crystal within the specimen or structure. The times to rupture under monotonous creep conditions can differ from one orientation to another by an order of two decimal places. Therefore, any three-dimensional modelling must necessarily take into account the strong anisotropy of the behaviour.

In the literature basically two different methods are applied to model the three-dimensional creep behaviour of single crystals. One of them is to use the different classes of *slip systems* and to formulate uniaxial creep equations for them. The advantage is that these equations are much less complicated than the three-dimensional ones, and the assemblage of all slip systems assures a three-dimensional law that automatically secures the symmetry of the crystal. Interactions between the different slip systems seem to be important and enter solely due to the work-hardening law, namely by the cross-hardening parameters. The validity of this approach, however, is rather limited. In certain temperature regimes, the creep behaviour is dominated by diffusional creep, which has nothing to do with slip system mechanisms. For this reason slip system approaches turn out to be inadequate for creep modelling within these regimes [21, 22].

The other approach, which is favoured in the present paper, makes use of representations by *tensor functions*, which are well known from linear algebra. The problem of this approach, which is by no means trivial, lies mainly in the task of giving the resulting constants and variables a physical interpretation.

We will limit our considerations to the primary and secondary creep, excluding the tertiary creep phase, because little is known about three-dimensional anisotropic continuum damage. The uniaxial model, however, has been successfully enlarged by a Kachanov-type damage parameter, which also describes tertiary creep till rupture (see [23]).

4.2. Modelling by a viscoelastic differential equation

The starting point for the present approach is the uniaxial modelling of the monotonous primary and secondary creep behaviour under tensile loadings in the [0 0 1]-orientation. This has been successfully done by means of a 4-parameter differential equation

$$\sigma^{\cdot\cdot} + A_1\sigma^{\cdot} + A_2\sigma = A_3\varepsilon^{\cdot\cdot} + A_4\varepsilon^{\cdot}, \tag{4.1}$$

where the four coefficients $A_{1,2,3,4}$ depend solely on the stress σ, which is indeed constant

for creep tests. This dependence has been specified by means of a linear function

$$f(\sigma) = K_1 - K_2\sigma, \quad \text{with} \quad K_{1,2} > 0, \tag{4.2}$$

such that

$$\begin{aligned} A_1 &= A_{01}/f(\sigma), \\ A_2 &= A_{02}/f(\sigma)^2, \\ A_3 &= A_{03}, \\ A_4 &= A_{04}/f(\sigma), \end{aligned}$$

where the A_{0i} are material constants for isothermal processes. This form of dependence is equivalent to the introduction of an artificial time (see [23]). The applicability of this expression, however, is limited to a certain interval, where $f(\sigma)$ is positive. A more appropriate form of this dependence is

$$f(\sigma) = K_3 \exp(-K_4\sigma), \quad \text{with} \quad K_{3,4} > 0. \tag{4.3}$$

This function renders positive values in the whole (tension) stress regime.

The numerical integration of Eq. (4.1) can be easily done by introducing an internal variable and reducing the differential equation to a system of first order differential equations. Appropriate initial conditions for such variable result from its physical interpretation.

The three-dimensional generalization is a reinterpretation of Eq. (4.1) in the following way:

σ: the stress tensor $\mathbf{S}$,

ε: the (infinitesimal) strain tensor $\mathbf{E}$,

$A_{1,2,3,4}$: 4th rank tensors $\mathbf{A}_{1,2,3,4}$, fulfilling the cubic anisotropy conditions of the crystal.

The differential equation now reads

$$\mathbf{S}'' + \mathbf{A}_1\mathbf{S}' + \mathbf{A}_2\mathbf{S} = \mathbf{A}_3\mathbf{E}'' + \mathbf{A}_4\mathbf{E}'. \tag{4.4}$$

For the 4th rank tensors a complete cubic representation is known from linear algebra (see [24, 25, 26]) as a linear combination of 3 structural tensors

$$\mathbf{A}_i = \alpha_{i1}\mathbf{P}_1 + \alpha_{i2}\mathbf{P}_2 + \alpha_{i3}\mathbf{P}_3 \tag{4.5}$$

given by

$$\begin{aligned} \mathbf{P}_1 &:= 1/3\ \mathbf{1} \otimes \mathbf{1}, \\ \mathbf{P}_2 &:= \sum_{i=1}^{3} \mathbf{e}_i \otimes \mathbf{e}_i \otimes \mathbf{e}_i \otimes \mathbf{e}_i - \mathbf{P}_1, \\ \mathbf{P}_3 &:= \mathbf{I} - \mathbf{P}_1 - \mathbf{P}_2, \end{aligned}$$

where $\mathbf{e}_i$ denotes the lattice directors, $\mathbf{1}$ the second rank identity, $\mathbf{I}$ the fourth rank identity, and $\otimes$ the tensorial product. α_{ij} are $4 \times 3 = 12$ (stress-dependent) material constants.

The stress dependence of these constants is assumed to be of an analogous form to Eq. (4.3). Instead of the (unique) tension stress in the uniaxial case, we need an expression for the stress intensity, which is invariant under cubic symmetry transformations. A complete integrity base for the specific symmetry group is given by the nine invariants (see [27])

$$\begin{aligned} J_1 &= \mathrm{tr}(\mathbf{S}), \\ J_2 &= 1/2[\mathrm{tr}^2(\mathbf{S}) + \mathrm{tr}(\mathbf{S}^2)], \end{aligned}$$

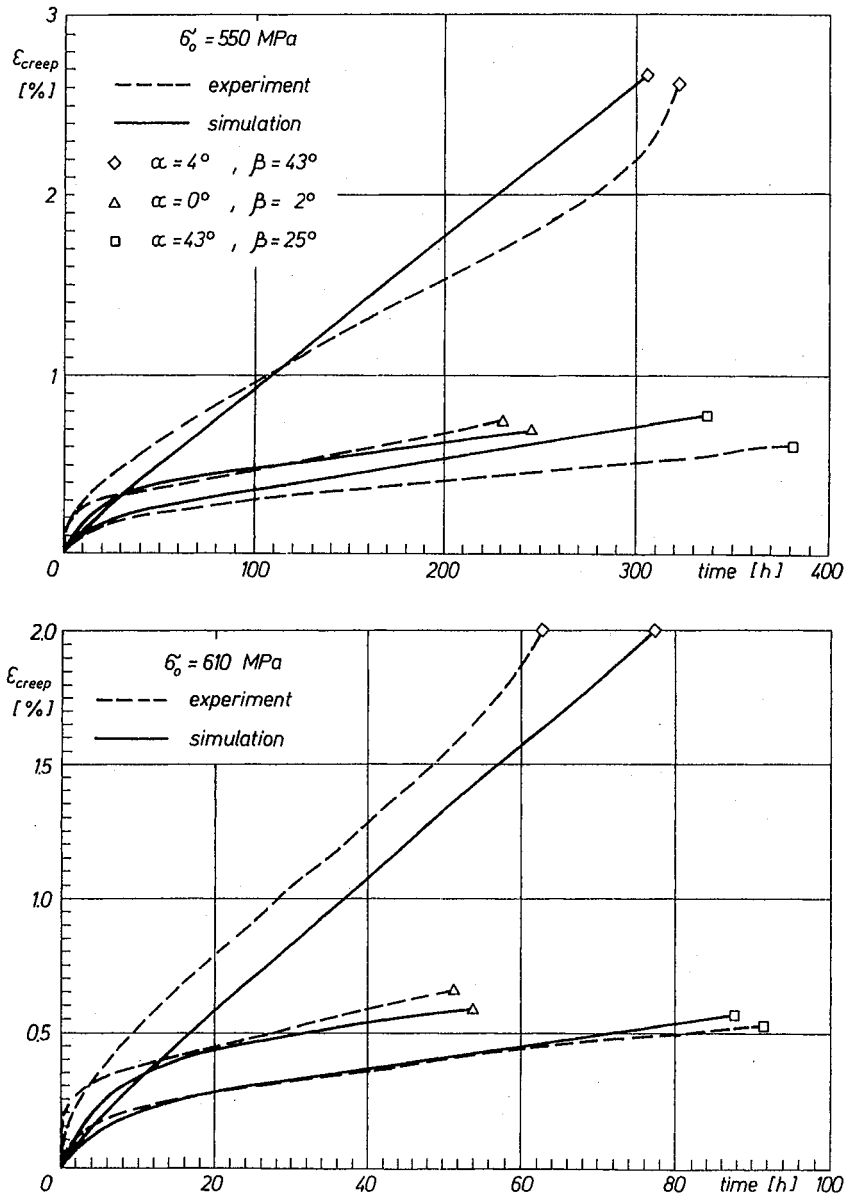

FIG. 5. Modelling of creep behaviour of a single crystal at different orientations, α and β are the first and second Eulerian angles.

$$J_3 = \det(\mathbf{S}),$$

$$J_4 = \sigma_{12}^2 + \sigma_{23}^2 + \sigma_{31}^2,$$

$$J_5 = \sigma_{12}\sigma_{23}\sigma_{31},$$

$$J_6 = (\sigma_{11} + \sigma_{22})\sigma_{12}^2 + (\sigma_{22} + \sigma_{33})\sigma_{23}^2 + (\sigma_{33} + \sigma_{11})\sigma_{31}^2,$$

$$J_7 = \sigma_{12}^2\sigma_{23}^2 + \sigma_{23}^2\sigma_{31}^2 + \sigma_{31}^2\sigma_{12}^2,$$
$$J_8 = \sigma_{11}\sigma_{12}^2\sigma_{31}^2 + \sigma_{22}\sigma_{23}^2\sigma_{12}^2 + \sigma_{33}\sigma_{31}^2\sigma_{23}^2,$$
$$J_9 = \sigma_{11}\sigma_{22}\sigma_{12}^2 + \sigma_{22}\sigma_{33}\sigma_{23}^2 + \sigma_{33}\sigma_{11}\sigma_{31}^2.$$

For our purposes the following ansatz-functions turned out to be appropriate:

$$f_i(\mathbf{S}) = K_{i1}\exp(-K_{i2}J_2 - K_{i3}J_4 - K_{i4}J_5 - K_{i5}J_6), \quad \text{with} \quad K_{ij} > 0. \tag{4.6}$$

The number of the material constants can be reduced to 17 by assuming the inelastic incompressibility, as usual. The remaining set of material constants has been calibrated by the least square methods to tensile creep tests in different orientations. In Fig. 5 the results of an adjustment by a single set of parameters is shown for the single crystal superalloy CMSX6 at 760° C. The tests have been performed by Siemens-KWU. α and β are the first and second Eulerian angles, which determine the orientation of the crystal within the samples.

5. Conclusions

The inelastic deformation behaviour of particle hardened superalloys such as e.g. IN 738 LC has different microstructural origins dependent on both the temperature and the strain-rate applied. It was shown that phenomenological constitutive equations like those of the viscoplastic Chaboche model are able to simulate the inelastic response of this class of materials under uniaxial as well as multiaxial loadings. Furthermore, the need of an additional temperature-rate term in the evolution equation for isotropic hardening is established if non-isothermal loadings have to be considered. Even then, only isothermal uniaxial tests are, in the investigated loading range, necessary to calibrate the model.

The modelling of the primary and secondary creep behaviour of single crystals is based on a four-parameter differential equation with stress-dependent coefficients. The three-dimensional generalization uses representations of tensor functions performing the required material symmetries of a f.c.c. crystal. The orientation dependence of creep behaviour is reproduced by this model, as comparison with experiments shows.

Acknowledgements

The authors are grateful for the financial support of the Deutsche Forschungsgemeinschaft (DFG) within the Sonderforschungsbereich 339 of the Technical University Berlin. The contribution of Drs. J. MEERSMANN, J. ZIEBS and Mr. H.-J. KÜHN at the laboratory for mechanical testing (BAM-1.21) in performing the experimental work is gratefully acknowledged.

The single crystal part has been funded by Siemens-KWU within COST-Round II WP 501, which is gratefully acknowledged.

References

1. J.-L. CHABOCHE, *Viscoplastic constitutive equations for the description of cyclic anisotropic behaviour of metals*, Bull. de l'Academie des Sciences, Serie des Techniques, **25**, 33–42, 1977.
2. D.P. POPE and S.S. EZZ, *Mechanical properties of* Ni_3Al *and nickel-base alloys with high volume fraction of* γ', Internat. Metals Reviews, **29**, 3, 136–167, 1984.

3. D.N. ROBINSON, *On thermo-mechanical testing in support of constitutive equation development for high-temperature application*, Lewis Research Center, NASA-CR 174879, 1985.
4. E. KREMPL, *Models of viscoplasticity, some comments on equilibrium (back) stress and drag stress*, Acta Mech., **69**, 25–42, 1987.
5. O.T. BRUHNS *et al.*, *A comparative study of unified constitutive equations for modelling inelastic material behaviour*, [in:] Proc. Post-SMiRT Seminar No 5 on Inelastic Analysis, Fatigue and Life Prediction, Paris, 1993.
6. S.R. BODNER, *Review of a unified elastic-viscoplastic theory*, [in:] Unified Constitutive Equations for Creep and Plasticity, A.K. MILLER [Ed.], Elsevier Applied Science, 273–301, 1987.
7. J. OLSCHEWSKI, R. SIEVERT and A. BERTRAM, *A comparison of the predictive capabilities of two unified constitutive models at elevated temperatures*, [in:] Constitutive Laws of Engineering Materials, C.S. DESAI *et al.* [Eds.] ASME PRESS, 775–758, 1991.
8. J.J. MORE, *The Levenberg-Marquardt algorithm: implementation and theory* [in:] Numerical Analysis, G.A. WATSON [Ed.], Lecture Notes in Mathematics 630, A.D. DOLD, B. ECKMANN [Eds.], Springer-Verlag, Berlin, 105–116, 1978.
9. J. ZIEBS, J. MEERSMANN and H.-J. KÜHN, *Effects of proportional and non-proportional straining sequences on hardening/softening behavior of IN 738 LC at elevated temperatures* [in:] Multiaxial Plasticity, A. BENALLAL *et al.* [Eds.], MECAMAT'92, Laboratoire de Mechanique et Technologie, Cachan–France, 224–255, 1992.
10. K.S. CHAN, U.S. LINDHOLM, S.R. BODNER and A. NAGY, *High temperature inelastic deformation of the B1900+Hf alloy under multiaxial loading: theory and experiment*, J. Engng. Mat. Technology, **112**, 7–14, 1990.
11. A. BENALLAL and A. BEN CHEIKH, *Constitutive equations for anisothermal elasto-viscoplasticity* [in:] Constitutive Laws for Engineering Materials, C.S. DESAI *et al.* [Eds.], 667–674, 1987.
12. V.S. BHATTACHAR and D.C. STOUFFER, *Constitutive equations for the thermomechanical response of Rene'80: Part 1, 2*, J. Engng. Mat. Technology, **115**, 351–364, 1993.
13. V. MORENO and E.H. JORDAN, *Prediction of material thermomechanical response with a unified viscoplastic constitutive model*, Int. J. Plasticity, **2**, 223–245, 1986.
14. D. SLAVIK and H.A. SEHITOGLU, *A constitutive model for high temperature loading: Part I, II* [in:] Thermal Stress, Material Deformation and Thermo-Mechanical Fatigue, H. SEHITOGLU, S.Y. ZAMRIK [Eds.] ASME, PVP-123, 65–83, 1987.
15. A. BENALLAL and A. BEN CHEIKH, *Damage and rupture of viscoplastic structures under anisothermal cyclic loadings*, [in:] High Temperature Fracture Mechanisms and Mechanics, EGF6, P. BENSUSSAN [Ed.] MEP, 227–247, 1990.
16. D.L. MCDOWELL, *A nonlinear kinematic hardening theory for cyclic thermo-plasticity and thermoviscoplasticity*, Int. J. Plasticity, **8**, 695–728, 1992.
17. J.-L. CHABOCHE, *Thermodynamically based viscoplastic constitutive equations: theory versus experiment*, [in:] High Temperature Constitutive Modeling — Theory and Application, A.D. FREED, K.P. WALKER [Eds.], ASME, MD-Vol. 26, AMD-Vol. 121, 207–226, 1991.
18. E. KREMPL, *Isotropic viscoplasticity theory based on overstress for small strain*, presented at the 6th Polish-German Symposium on Mechanics on Inelastic Solids and Structures, Czerniejewo, Poland, 1993.
19. R. SIEVERT, C. HAFTAOGLU and J. OLSCHEWSKI, *Verifizierung und Weiterentwicklung von zwei viskoplastischen Stoffmodellen für Teilchen-härtende Nickelbasis-Legierungen auf der Grundlage ein- und mehrachsiger thermisch-mechanischer Versuche* [in:] Forschungsbericht 1990–1992 des Sfb 339, TU Berlin, 407–443, 1993.
20. J. LEMAITRE and J.-L. CHABOCHE, *Mechanics of solid materials*, Cambridge University Press, 1990.
21. R.A. MACKAY and R.D. MAIER, *The influence of orientation on the stress rupture properties of nickel-base superalloy single crystals*, Metall. Trans., **13A**, 1747–1754, 1982.
22. D.J. SHAH, *Orientation dependence of creep behavior of single crystal* $\gamma'(Nu_3Al)$, Scripta Metallurgica, **17**, 8, 997–1002, 1983.
23. A. BERTRAM, J. OLSCHEWSKI, M. ZELEWSKI and R. SIEVERT, *Anisotropic creep modeling for f.c.c. single crystals* [in:] Creep in Structures, IUTAM Symposium Cracow/Poland 1990, M. ŻYCZKOWSKI [Ed.], Springer-Verlag, Berlin, 1991.
24. A. BERTRAM, J. OLSCHEWSKI, R. SIEVERT and M. ZELEWSKI, *Constitutive modeling of the creep behaviour of single crystals with applications to notched specimens* [in:] Constitutive Laws for Engineering Materials, C.S. DESAI *et al.* [Eds.], ASME Press, New York 1991.
25. A. BERTRAM and J. OLSCHEWSKI, *Formulation of anisotropic linear viscoelastic constitutive laws by a projection method* [in:] High Temperature Constitutive Modeling — Theory and Application, A. FREED, K.P. WALKER

[Eds.], ASME, MD-Vol. 26, AMD-Vol., 121, 129–137, 1991.
26. A. BERTRAM and J. OLSCHEWSKI, *Zur Formulierung anisotroper linearer anelastischer Stoffgleichungen mit Hilfe einer Projektionsmethode*, ZAMM, **73**, 4–5, T401-T403, 1993.
27. G.F. SMITH and E. KIRAL, *Integrity bases for N symmetric second-order tensors — the crystal classes*, Rend. Circ. Mat. Palermo II, Ser. **18**, 5–22, 1959.

BUNDESANSTALT FÜR MATERIALFORSCHUNG AND — PRÜFUNG (BAM) BERLIN, GERMANY.

Received January 3, 1994.